Correspondence

Beam-Domain Eigenspace-Based Minimum Variance Beamformer for Medical Ultrasound Imaging

Xing Zeng, Yuanyuan Wang, *Senior Member, IEEE*, Jinhua Yu, and Yi Guo

***Abstract*—The eigenspace-based minimum variance (ESBMV) beamformer can provide good imaging resolution and contrast; however, the performance is achieved at the cost of high computational complexity. In adaptive array processing, the beamspace method is an efficient way to lower the computational complexity. In this paper, we combine the beamspace method with the ESBMV beamformer and propose a beam-domain ESBMV beamformer. We demonstrate the feasibility of introducing the beamspace into the ESBMV beamformer and propose an effective method of forming the transform matrix based on the spatial spectrum of the array signals. We also illustrate the performance of the proposed beamformer when resolving point scatterers and a cyst phantom with both simulated and experimental data. The results show that the proposed method can achieve performance comparable to the ESBMV beamformer within much shorter time.**

I. Introduction

In medical ultrasound imaging, beamforming is conventionally carried out by the delay-and-sum (DAS) method. Because it uses predefined and data-independent weights, the DAS beamformer is weak in suppressing interference and noise, resulting in relatively poor imaging resolution and contrast. To improve the imaging resolution, adaptive beamformers were introduced into medical ultrasound imaging. Among these adaptive beamformers, the minimum variance (MV) beamformer, originally introduced by Capon in 1969 [1], is a widely used method. The weights of the MV beamformer are calculated by minimizing the power of the beamformer output subject to the constraint that the response from the focus point is passed without distortion. Several researchers have investigated the MV beamformer during the past decades. Mann [2] proposed the Frost beamformer. Sasso and Cohen-Bacire [3] introduced the spatial smoothing technique to obtain a well-conditioned covariance matrix. Synnevåg *et al.* applied the diagonal loading [4] technique in the estimation of the covariance matrix to ensure its robustness. Holfort *et al.* implemented the MV beamformer in the frequency domain and proposed the broad-MV beamformer [5]. In addition, coherence-factor methods have also been investigated to improve the performance of MV beamformer [6], [7].

Previous works have shown that the MV beamformer offers a better resolution than the DAS beamformer. However, the improvement for imaging contrast is not as significant as for resolution [8]. Hence, eigenspace-based methods have been proposed. These methods utilize the orthogonal property of the signal and the noise subspace constructed by the eigenvectors of the covariance matrix [9]. The signal subspace represents the information of the main lobe signals, whereas the noise subspace is related to the side lobe signals. In the eigenspace-based minimum variance (ESBMV) beamformer proposed by Asl and Mahloojifar [8], the weights are optimized by projecting the MV weights onto the constructed signal subspace. In this way, the contribution of the side lobe signals can be greatly reduced, but the contribution of the main lobe signals remains, which leads to a significant improvement in imaging resolution and contrast [10], [11].

However, the eigen-decomposition of the covariance matrix adds many calculations. Although the computational overheads brought by the eigen-decomposition and inversion of the covariance matrix are both cubic with the array size, $O(L^3)$, the coefficient before the cubic term is much bigger in eigen-decomposition than in inversion. Therefore, it is necessary to lower the computational complexity of the ESBMV beamformer.

The study of the low-complexity adaptive beamformer has been an area of great interest in ultrasound imaging. Several methods have been proposed. A direct method is reducing the number of array elements used to emit or receive the echo waves, such as the method proposed by Vignon and Burcher [12]. However, this method either affects the imaging resolution or makes the beamformer susceptible to signal cancellation because of lack of spatial smoothing. Another low-complexity beamformer was proposed by Synnevåg *et al.* [13]. In this method, the weights of the beamformer leading to the lowest output power are selected from a predefined set of distortionless weights. However, because the best weights may be different for different scenarios, the performance of this method depends very much on the window design [13]. In [14], Asl and Mahloojifar applied the Toeplitz structure into estimating the covariance matrix. The computational loads can be reduced from $O(L^3)$ to $O(L^2)$ using the fast algorithm for the inversion of the Toeplitz matrix.

Because the calculation of the ESBMV weights involves not only the inversion but also the eigen-decomposition of the covariance matrix, the improvement brought by the

Manuscript received April 25, 2013; accepted September 12, 2013. This work is supported by the National Natural Science Foundation of China (grant numbers 61271071 and 11228411), the National Key Technology R&D Program of China (grant number 2012BAI13B02), and the Specialized Research Fund for the Doctoral Program of Higher Education of China (grant number 20110071110017).

The authors are with the Department of Electronic Engineering, Fudan University, Shanghai, China (e-mail: yywang@fudan.edu.cn).

DOI http://dx.doi.org/10.1109/TUFFC.2013.2866

Toeplitz structure is limited. In [15], Nilsen and Hafizovic applied the beamspace method to the Capon beamformer and successfully achieved reduced computational complexity with performance comparable to the ordinary Capon beamformer. In this method, the array signals are transformed to a reduced-dimensional beamspace. In this way, the inversion and eigen-decomposition can both be calculated with the reduced-dimensional covariance matrix, which is suitable for the ESBMV beamformer.

In this paper, we apply the beamspace algorithm to the ESBMV beamformer and propose the beam-domain ESBMV (B-ESBMV) beamformer. To decrease the acquisition time of the echo ultrasound wave, we use plane-wave emission [16] acquisitions as the emission method, in which the whole region can be covered with a single emission. Several beamformers have been proposed based on plane-wave acquisitions. One of the most interesting methods is the one presented by Lu [17], in which the beamforming of a plane wave is evaluated in a 2-D Fourier domain. Kruizinga *et al.* proposed an improved algorithm using the nonuniform fast Fourier transform (NUFFT) [18]. These works indicate the great potential of the plane-wave method in low-complexity beamforming. To investigate the performance and the execution time of the B-ESBMV beamformer, point scatterers and a cyst phantom are simulated. The results show that the B-ESBMV beamformer can achieve almost the same performance of the ESBMV beamformer within time even shorter than the MV beamformer.

The outline of this manuscript is as follows. The background is presented in Section II, including the signal sensor model, the MV, and the ESBMV beamformer. The method of the proposed beamformer is introduced in Section III. The imaging results of the different beamformers are shown in Section IV. Finally, the execution time is discussed in Section V and conclusions are given in Section VI.

II. Background

A. Minimum Variance Beamformer

For a linear array of M elements, the signal received at the time instant k can be given by

$$\mathbf{x}(k) = s(k)\mathbf{a} + \mathbf{p}(k), \tag{1}$$

where $s(k)$ is the desired signal, $\mathbf{p}(k)$ is the sum of interference and noise, and $\mathbf{a}$ is the steering vector corresponding to the desired signal.

The weights of the MV beamformer are obtained by minimizing the power of the beamformer output under the constraint that the signal reflecting from the imaging point is passed without distortion:

$$\mathbf{w}_{\mathrm{MV}} = \underset{\mathbf{w}}{\operatorname{argmin}}\, \mathbf{w}^{\mathrm{H}}\mathbf{R}\mathbf{w} \quad \text{subject to } \mathbf{w}^{\mathrm{H}}\mathbf{a} = 1, \tag{2}$$

where $\mathbf{R}$ is the covariance matrix. Then, the weights of the MV beamformer are given by

$$\mathbf{w}_{\mathrm{MV}} = \frac{\mathbf{R}^{-1}\mathbf{a}}{\mathbf{a}^{\mathrm{H}}\mathbf{R}^{-1}\mathbf{a}}. \tag{3}$$

In practice, the covariance matrix is usually estimated by the sample covariance matrix. To get a well-conditioned matrix, spatial smoothing [3] is used, in which the array is divided into overlapping subarrays and the covariance matrixes obtained from all subarrays are averaged to form the covariance matrix:

$$\mathbf{R} = \frac{1}{Q}\sum_{q=1}^{Q}\mathbf{x}_q\mathbf{x}_q^{\mathrm{H}}, \tag{4}$$

where $Q = M - L + 1$ is the number of overlapped subarrays, L is the length of a subarray, and $\mathbf{x}_q = [x_q(k), x_{q+1}(k), \ldots, x_{q+L-1}(k)]^{\mathrm{T}}$ is the signal vector of the qth subarray. The diagonal loading technique is also used, in which a constant is added into the diagonal elements of the covariance, $\mathbf{R}_{\mathrm{DL}} = \mathbf{R} + \varepsilon\mathbf{I}$, where $\mathbf{I}$ is the identity matrix and ε is the diagonal loading factor. The loading factor ε can be set to be δ times the power of the received signals [4]:

$$\varepsilon = \delta \cdot \mathrm{trace}\{\mathbf{R}\}. \tag{5}$$

B. Eigenspace-Based Minimum Variance Beamformer

In the ESBMV beamformer, the covariance matrix is eigen-decomposed to two orthogonal subspaces:

$$\begin{aligned}\mathbf{R} = \mathbf{U}\Lambda\mathbf{U}^{\mathrm{H}} &= \sum_{i=1}^{L}\lambda_i\mathbf{v}_i\mathbf{v}_i^{\mathrm{H}} = \mathbf{U}_{\mathrm{s}}\Lambda_{\mathrm{s}}\mathbf{U}_{\mathrm{s}}^{\mathrm{H}} + \mathbf{U}_{\mathrm{p}}\Lambda_{\mathrm{p}}\mathbf{U}_{\mathrm{p}}^{\mathrm{H}} \\ &= \sum_{i=1}^{N_{\mathrm{sig}}}\lambda_i\mathbf{v}_i\mathbf{v}_i^{\mathrm{H}} + \sum_{i=N_{\mathrm{sig}}+1}^{L}\lambda_i\mathbf{v}_i\mathbf{v}_i^{\mathrm{H}} = \mathbf{R}_{\mathrm{s}} + \mathbf{R}_{\mathrm{p}},\end{aligned} \tag{6}$$

where $\mathbf{\Lambda} = \mathrm{diag}[\lambda_1, \lambda_1, \ldots, \lambda_L]$, $\lambda_1 \geq \lambda_2 \geq \ldots \geq \lambda_L$ are the eigenvalues in descending order, and $\mathbf{U} = [\mathbf{v}_1, \mathbf{v}_2, \ldots, \mathbf{v}_L]$ consists of the orthonormal eigenvector $\mathbf{v}_i$ $(i = 1, 2, \ldots, L)$ corresponding to λ_i. Similarly, $\mathbf{U}_{\mathrm{s}}$ and $\mathbf{U}_{\mathrm{p}}$ are the signal subspace corresponding to the N_{sig} largest eigenvalues and the noise subspace corresponding to the remaining smaller eigenvalues.

Then, the ESBMV weights are calculated by projecting the MV weights onto the constructed signal subspace:

$$\mathbf{w}_{\mathrm{ESBMV}} = \mathbf{U}_{\mathrm{s}}\mathbf{U}_{\mathrm{s}}^{\mathrm{H}}\mathbf{w}_{\mathrm{MV}}. \tag{7}$$

Ideally, the signal subspace $\mathbf{U}_{\mathrm{s}}$ is orthogonal to the noise subspace $\mathbf{U}_{\mathrm{p}}$, so the noise output power can be greatly suppressed.

III. Method

A. Beam-Domain Eigenspace-Based Minimum Variance Beamformer

The main idea of the beamspace algorithm is combining the beam-domain signals instead of the array signals to form the beamformer output. The transformation from the array signals to the beam-domain signals is done by multiplying the array signals $\mathbf{x}$ with an $L \times L$ transform matrix $\mathbf{T}$, which is

$$\mathbf{x}_{\mathrm{B}} = \mathbf{T}\mathbf{x}. \tag{8}$$

Each row of the matrix $\mathbf{T}$ is a group of weights. In practice, the transform matrix $\mathbf{T}$ is always chosen to be the discrete Fourier transform (DFT) matrix, which satisfies $\mathbf{T}^{\mathrm{H}}\mathbf{T} = 1$.

In the same way as the array signals, the steering vector and the covariance matrix are also transformed from the array domain to the beam domain:

$$\begin{aligned} \mathbf{a}_{\mathrm{B}} &= \mathbf{T}\mathbf{a}; \\ \mathbf{R}_{\mathrm{B}} &= \mathbf{x}_{\mathrm{B}}\mathbf{x}_{\mathrm{B}}^{\mathrm{H}} = \mathbf{T}\mathbf{x}(\mathbf{T}\mathbf{x})^{\mathrm{H}} = \mathbf{T}\mathbf{R}\mathbf{T}^{\mathrm{H}}. \end{aligned} \tag{9}$$

It can be proved that the method of the ESBMV beamformer can be implemented in the beam domain. Together with (6), if we eigen-decompose the array-domain covariance matrix within the beam-domain covariance matrix, we will get

$$\begin{aligned} \mathbf{R}_{\mathrm{B}} &= \mathbf{T}\mathbf{R}\mathbf{T}^{\mathrm{H}} = \mathbf{T}\mathbf{U}\Lambda\mathbf{U}^{\mathrm{H}}\mathbf{T}^{\mathrm{H}} = \mathbf{T}\left(\sum_{i=1}^{L}\lambda_i\mathbf{v}_i\mathbf{v}_i^{\mathrm{H}}\right)\mathbf{T}^{\mathrm{H}} \\ &= \mathbf{T}\mathbf{U}_{\mathrm{s}}\Lambda_{\mathrm{s}}\mathbf{U}_{\mathrm{s}}^{\mathrm{H}}\mathbf{T}^{\mathrm{H}} + \mathbf{T}\mathbf{U}_{\mathrm{p}}\Lambda_{\mathrm{p}}\mathbf{U}_{\mathrm{p}}^{\mathrm{H}}\mathbf{T}^{\mathrm{H}} \\ &= \sum_{i=1}^{N_{\mathrm{sig}}}\lambda_i\mathbf{T}\mathbf{v}_i(\mathbf{T}\mathbf{v}_i)^{\mathrm{H}} + \sum_{i=N_{\mathrm{sig}}+1}^{L}\lambda_j\mathbf{T}\mathbf{v}_j(\mathbf{T}\mathbf{v}_j)^{\mathrm{H}}. \end{aligned} \tag{10}$$

Because of the orthogonality between the eigenvectors, the eigenvectors $\mathbf{v}_i$ and $\mathbf{v}_j$ satisfy

$$\mathbf{v}_i^{\mathrm{H}}\mathbf{v}_i = 1, \mathbf{v}_j^{\mathrm{H}}\mathbf{v}_j = 1, \mathbf{v}_i^{\mathrm{H}}\mathbf{v}_j = 0. \tag{11}$$

Because the transform matrix $\mathbf{T}$ is unitary matrix, the decomposition products $\mathbf{T}\mathbf{v}_i$ $(i = 1, 2, \ldots, L)$ in (10) are orthogonal to each other:

$$\begin{aligned} &(\mathbf{T}\mathbf{v}_i)^{\mathrm{H}}\mathbf{T}\mathbf{v}_i = \mathbf{v}_i^{\mathrm{H}}\mathbf{I}\mathbf{v}_i = 1, \quad (\mathbf{T}\mathbf{v}_j)^{\mathrm{H}}\mathbf{T}\mathbf{v}_j = \mathbf{v}_j^{\mathrm{H}}\mathbf{I}\mathbf{v}_j = 1, \\ &(\mathbf{T}\mathbf{v}_i)^{\mathrm{H}}\mathbf{T}\mathbf{v}_j = \mathbf{v}_i^{\mathrm{H}}\mathbf{I}\mathbf{v}_j = 0, \end{aligned} \tag{12}$$

which means that the vectors $\mathbf{T}\mathbf{v}_i$ $(i = 1, 2, \ldots, L)$ are the eigenvectors of $\mathbf{R}_{\mathrm{B}}$ corresponding to the eigenvalue λ_i. Then, the signal subspace and the noise subspace of $\mathbf{R}_{\mathrm{B}}$ can be simply calculated by the array-domain signal subspace and noise subspace as $\mathbf{T}\mathbf{U}_{\mathrm{s}}$ and $\mathbf{T}\mathbf{U}_{\mathrm{n}}$.

Finally, the weights of the B-ESBMV beamformer are given by

$$\mathbf{w}_{\text{B-ESBMV}} = \mathbf{T}\mathbf{U}_{\mathrm{s}}\mathbf{U}_{\mathrm{s}}^{\mathrm{H}}\mathbf{T}^{\mathrm{H}}\mathbf{w}_{\text{B-MV}}. \tag{13}$$

The B-ESBMV is formulated based on the same principle as the array-domain ESBMV beamformer. Therefore, the B-ESBMV beamformer can achieve the same performance as the ESBMV beamformer.

B. Construction of the Transform Matrix

If the transform matrix $\mathbf{T}$ is still a matrix with $L \times L$ dimension, $\mathbf{R}_{\mathrm{B}}$ has the same dimension as the $\mathbf{R}$, which means the computational loads caused are not reduced. To decrease the computational complexity of the ESBMV beamformer, some rows must be removed from the transform matrix. If the dimension of transform matrix $\mathbf{T}$ is set to be $P \times L$, the dimension of the covariance matrix can be reduced from $L \times L$ to $P \times P$. In this way, the ESBMV weights are not acquired by (13) using the array-domain signal subspace but by directly eigen-decomposing the beam-domain covariance matrix in the same way as (6). Then, the computational complexity of the inversion and eigen-decomposition can be reduced from $O(L^3)$ to $O(P^3)$. Of course, reducing the number of the beams will somehow affect the performance of the beamformer, so there should be a balance between the complexity and performance.

To maintain the general performance of the ESBMV beamformer, we utilize the useful property of the spatial spectrum of the array signals to form the transform matrix, which is similar to the method presented in [14]. The spatial spectrum is acquired by applying the 1-D Fourier transformation along the array elements in the lateral direction of the images. We shift the phase of the transform items to locate the dc component at the central spatial frequency with index $L/2$:

$$x_{\mathrm{s}}(k) = \sum_{i=0}^{L-1} x(i)e^{-j2\pi(k-(L/2))(i/L)}, \tag{14}$$

where $k = 0$ to $L - 1$ is the spatial frequency index. Fig. 1 shows the delayed echo waves from a focus point and a nearby interference source and their spatial spectra. After appropriate delays are applied to the array, the wave reflecting from the imaging point becomes a plane-wave injecting directly onto the array. We can see that most of the energy concentrates around the central spatial frequency at the focus point, whereas most of the energy concentrates at other frequencies away from the central spatial frequency at the interference source. Thus, to form the transform matrix, we can select the beams near the central spatial frequency which contribute more to the energy of the delayed signal. Because most of the energy of the beam is distributed in the low spatial frequencies, this transformation will not lose too much information.

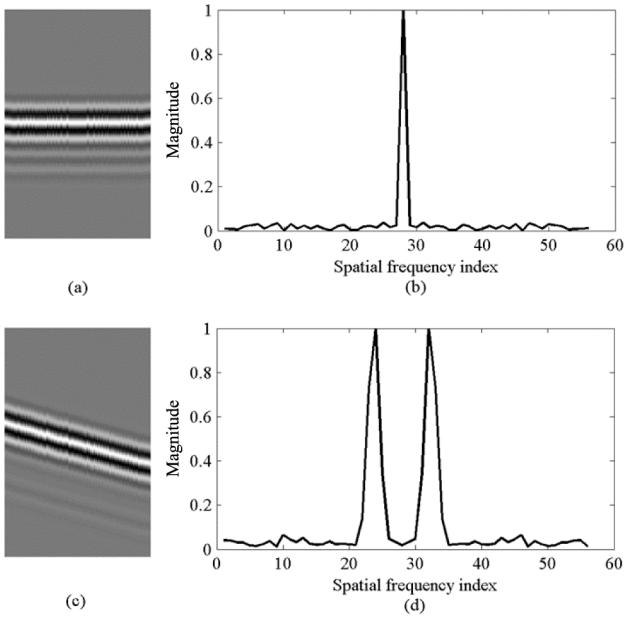

Fig. 1. (a) The echo wave from the focus point and (c) the echo wave from a nearby interference source after appropriate delays are applied to focus on the imaging point. The discrete Fourier spatial spectra of the echo waves are shown in (b) and (d). The central frequency of the spatial spectrum is at index $k = L/2 = 28$.

If the dimension of the transform matrix is set to be $(P + 1) \times L$, the elements in the matrix are given by

$$[\mathbf{T}]_{k,n} = \frac{1}{\sqrt{L}} e^{-j2\pi(k-(L/2))n/L}; \quad k = \frac{L-P}{2},\ldots,\frac{L}{2},\ldots,\frac{L+P}{2}; \quad n = 0,1,\ldots,L-1. \tag{15}$$

According to [19], the beams created by the each row in the matrix have their main response axes (MRA) in directions

$$\theta_k = \arcsin\left(2\left(k - \frac{L}{2}\right)/L\right); \quad k = \frac{L-P}{2},\ldots,\frac{L}{2},\ldots,\frac{L+P}{2}. \tag{16}$$

We can see that the MRAs are at angles from $\arcsin(-P/L)$ to $\arcsin(P/L)$, concentrating around 0°, which is the angle of the plane wave.

IV. Simulations and Results

In this section, we report simulations carried out to evaluate the performance of the proposed B-ESBMV beamformer in terms of the resolution and contrast using both simulated and experimental data. The simulated data were acquired with the ultrasound simulation phantom Field II [20].

A 7-MHz, 128-element linear array transducer with $\lambda/2$-spacing was used for the simulated data. The sampling rate was 100 MHz. A 5-MHz, 128-element linear array transducer with a pitch of 0.308 mm was used for the experimental data. The sampling rate was 40 MHz. A subarray size of $L = 48$ was used in the spatial smoothing and the loading factor δ was set to be 0.1 in the diagonal loading. The performances of the B-ESBMV beamformer with 11, 9, and 5 beams were demonstrated in comparison to the DAS, MV, broad-MV [5], and ESBMV beamformer. In all cases, the dynamic range was chosen to be 60 dB for a better display and comparison to the references.

A. Point Targets With Simulated Data

Eight point targets located at depths from 20 to 40 mm are simulated to study the resolution performance of the beamformers. The results are shown in Fig. 2. It can be seen that the B-ESBMV beamformers with 11 and 9 beams provide performance comparable to the ESBMV beamformer. The B-ESBMV beamformer with only 5 beams is a little worse because there are some artifacts around the targets. The performance of the imaging resolution is quantified using the full-width at half-maximum (FWHM) and peak-side-lobe (PSL) [5]. The PSL is defined as the peak value of the first side lobe. The results are given in Table I. The FWHMs and PSLs of the B-ESBMV beam-

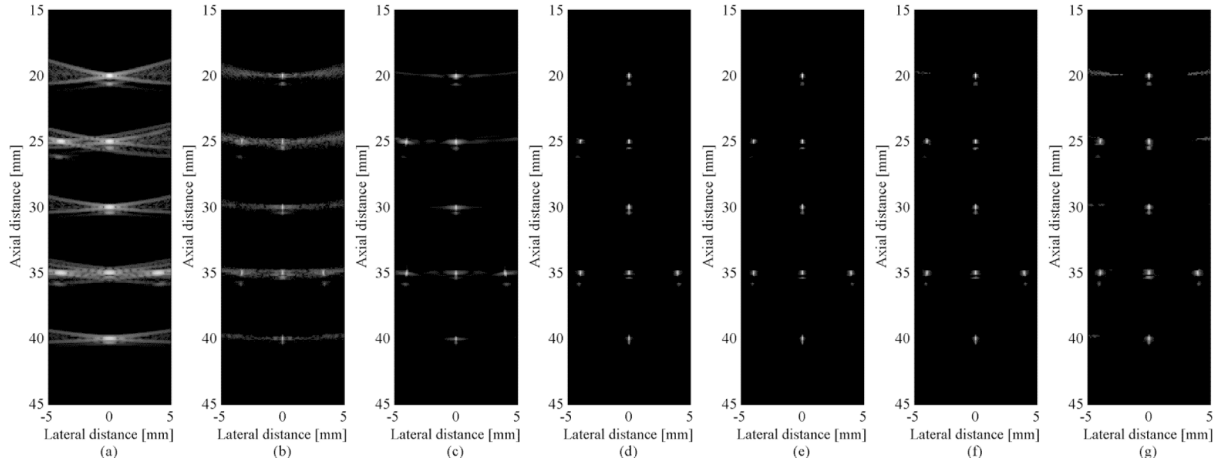

Fig. 2. Beamformed responses of 8 point targets. (a) DAS, (b) MV, (c) broad-MV, (d) ESBMV, (e) B-ESBMV with 11 beams, (f) B-ESBMV with 9 beams, (g) B-ESBMV with 5 beams.

TABLE I. FULL-WIDTH AT HALF-MAXIMUM (FWHM) AND PEAK SIDE LOBE (PSL) FOR DIFFERENT BEAMFORMERS AT $z = 20$ MM.

Beamformer	FWHM (mm)	PSL (dB)
DAS	0.22	−22.49
MV	0.06	−37.17
Broad-MV	0.06	−54.30
ESBMV	0.06	−95.24
B-ESBMV with 11 beams	0.06	−91.13
B-ESBMV with 9 beams	0.06	−89.61
B-ESBMV with 5 beams	0.08	−84.64

DAS = delay-and-sum; MV = minimum variance; ESBMV = eigenspace-based minimum variance; B-ESBMV = beam-domain eigenspace-based minimum variance.

formers with 11 and 9 beams are similar to the ESBMV beamformer and much better than the broad-MV, MV, and DAS beamformers. These results indicate that the B-ESBMV with only 9 beams can provide performance comparable to the ESBMV beamformer.

B. Cyst Phantom With Simulated Data

To demonstrate the performance of the proposed B-ESBMV beamformer in imaging contrast, three overlapping cysts in a speckle pattern were simulated. The cysts had a radius of 3 mm and centers at $(x, y, z) = (\pm 2, 0, 37)$ and $(0, 0, 33.5)$ mm. The beamformed images of the cyst phantom are shown in Fig. 3. We can see that the ESBMV beamformer and the B-ESBMV beamformer with 11 or 9 beams provide much better contrast than the broad-MV, MV, and DAS beamformers. The shape of the cysts is clear and the edge is easy to judge. The B-ESBMV beamformer with 5 beams is slightly worse than the ESBMV beamformer because the cyst is degraded by some artifacts. Here, the contrast ratio (CR) is used to evaluate the performance in imaging contrast, which is defined as the ratio of the mean value in the background to the mean value in the cyst region [21]. The results are shown in Table II. We can see that the ESBMV and the B-ESBMV beamformer with 11 and 9 beams have imaging contrasts similar to the ESBMV beamformer.

C. Cyst Phantom With Experimental Data

The data of a practical anechoic cyst was used for simulations as well. The cyst has a diameter of 6.7 mm and is centered at $(x, y, z) = (1.1, 0, 17.5)$ mm. The beamformed images are shown in Fig. 4, with a dynamic range of 60 dB. Obviously, the ESBMV and the B-ESBMV beamformer with 11 and 9 beams have much better imaging results than the broad-MV, MV, and DAS beamformers. Similarly, we use the CR to quantify the performance of all the beamformers in imaging contrast. The results are shown in Table III, providing the same conclusion as Table II.

V. DISCUSSION

The computational complexities of all beamformers are evaluated in theory here. The length of the subarray used in spatial smoothing is chosen to be 48 to ensure the high imaging resolution of the MV and ESBMV beamformer and the number of beams is chosen to be 9. The inversion of the covariance matrix involves $2L^3/3$ floating operations using the Gaussian elimination and the eigen-decomposition of the covariance matrix involves $21L^3$ floating operations using the Golub–Reinsch algorithm [22]. If we ignore the other calculations, the ESBMV beamformer needs $2/3 \times 48^3 + 21 \times 48^3 = 2\,396\,160$ floating operations to calculate the weights of a point. In the B-ESBMV beamformer,

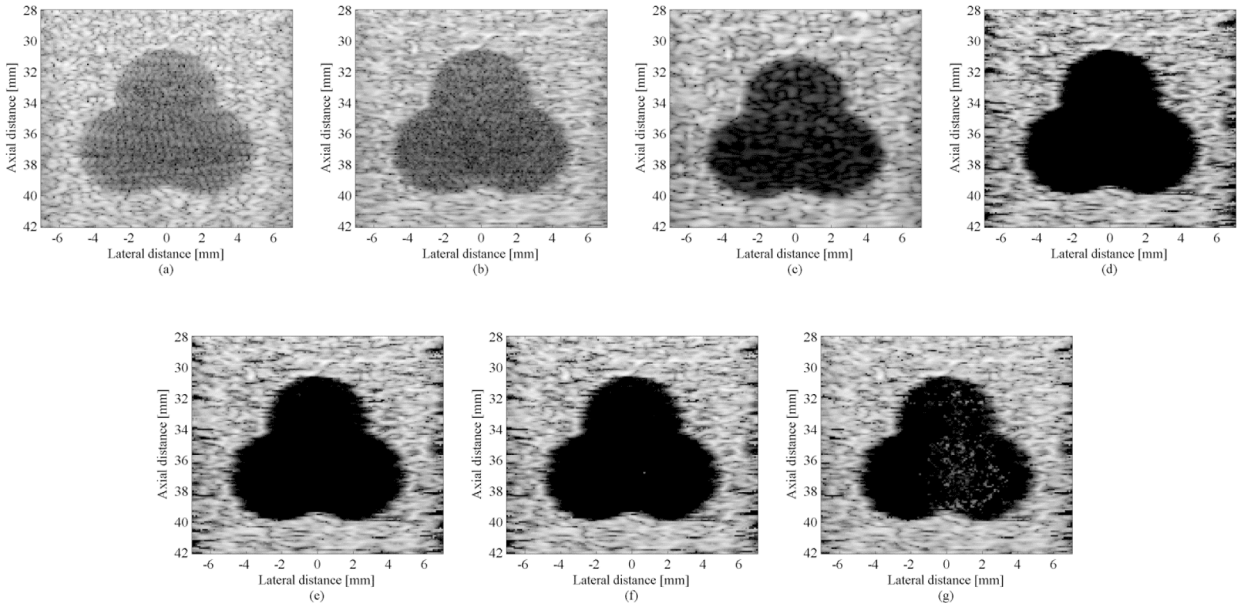

Fig. 3. Simulated beamformed responses of three overlapping cysts. (a) DAS, (b) MV, (c) broad-MV, (d) ESBMV, (e) B-ESBMV with 11 beams, (f) B-ESBMV with 9 beams, (g) B-ESBMV with 5 beams.

TABLE II. CONTRAST RATIO (CR) OF THE SIMULATED CYST FOR ALL BEAMFORMERS.

Beamformer	Mean intensity inside the cyst (dB)	Mean intensity outside the cyst (dB)	CR (dB)
DAS	−31.79	−14.55	17.24
MV	−37.37	−16.90	20.47
Broad-MV	−47.66	−16.54	31.12
ESBMV	−59.97	−21.04	38.93
B-ESBMV (11 beams)	−59.91	−20.99	38.92
B-ESBMV (9 beams)	−59.90	−20.62	39.28
B-ESBMV (5 beams)	−57.87	−19.51	38.36

DAS = delay-and-sum; MV = minimum variance; ESBMV = eigenspace-based minimum variance; B-ESBMV = beam-domain eigenspace-based minimum variance.

TABLE III. CONTRAST RATIO (CR) OF THE EXPERIMENTAL CYST FOR ALL BEAMFORMERS.

Beamformer	Mean intensity inside the cyst (dB)	Mean intensity outside the cyst (dB)	CR (dB)
DAS	−24.06	−18.28	5.78
MV	−25.74	−20.77	4.97
Broad-MV	−34.44	−22.67	11.77
ESBMV	−58.74	−27.71	31.03
B-ESBMV (11 beams)	−57.97	−26.98	30.99
B-ESBMV (9 beams)	−55.55	−26.76	28.79
B-ESBMV (5 beams)	−47.71	−25.88	21.83

DAS = delay-and-sum; MV = minimum variance; ESBMV = eigenspace-based minimum variance; B-ESBMV = beam-domain eigenspace-based minimum variance.

the inversion and eigen-decomposition take only $2/3 \times 9^3+21 \times 9^3 = 15\,795$ floating operations. The transformation from the array domain to the beam domain takes about $P \times L \times L = 26\,244$ floating operations. Therefore, it takes $26\,244 + 15\,795 = 42\,039$ floating operations in total, only 1.8% of the ESBMV beamformer. The DAS beamformer has a complexity of $O(M)$ (M is the array length and set to be 128). We can see that the complexity $O(P^3)$ of the B-ESBMV beamformer is not too much bigger than the DAS beamformer. Moreover, from [23] we observe that the complexity of eigen-decomposition can be decreased from $O(P^3)$ to $O(P^2)$ using recursive updating eigen-decomposition techniques. With this technique, the complexity of the B-ESBMV can be closer to that of the DAS beamformer. Together with the GPU acceleration, we believe that the proposed method has great potential for real-time use.

The time cost (mean ± standard deviation) for each beamformer is given in Table IV, together with the sizes of the images. The time is averaged through 10 tests. The time cost by the B-ESBMV beamformer with 9 beams is only 26.0% of the ESBMV beamformer and 79.5% of the MV beamformer in average. Because of the other calculations involved in the procedure of the B-ESBMV beamformer, such as the spatial smoothing and descending sort of the eigenvalues, the final improvements are not as

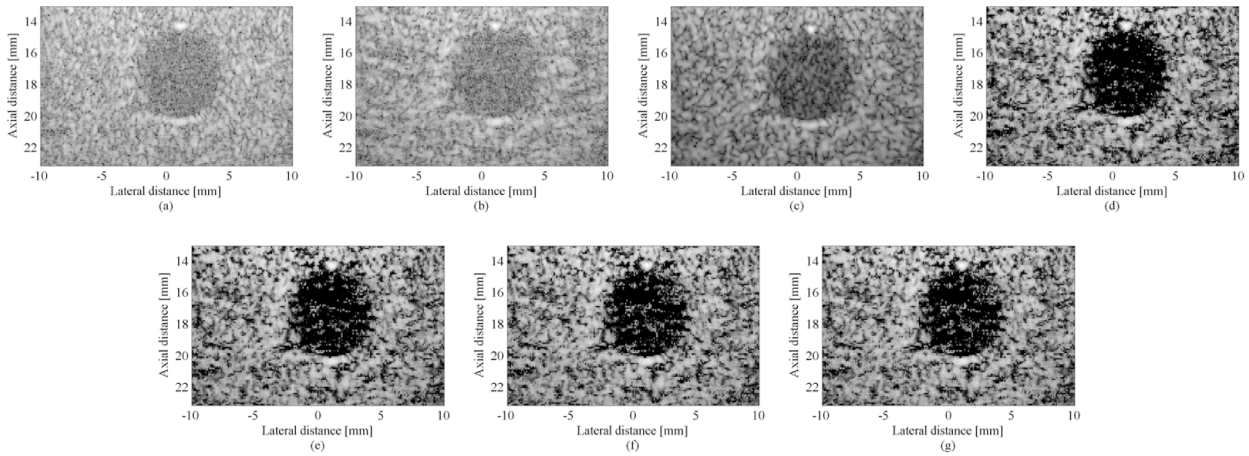

Fig. 4. Beamformed responses of real cyst phantom. (a) DAS, (b) MV, (c) broad-MV, (d) ESBMV, (e) B-ESBMV with 11 beams, (f) B-ESBMV with 9 beams, (g) B-ESBMV with 5 beams.

TABLE IV. TIME COST FOR ALL BEAMFORMERS (IN SECONDS).

Beamformer	Simulated scatterers (size: 301 × 101)	Simulated cyst (size: 141 × 141)	Experimental cyst (size: 101 × 201)
DAS	5.8220 ± 0.0432	3.7500 ± 0.0159	3.8080 ± 0.0277
MV	22.5240 ± 1.2305	15.2110 ± 0.1843	15.3560 ± 0.6526
Broad-MV	776.4992 ± 13.1797	492.4947 ± 12.7202	508.9044 ± 10.0621
ESBMV	68.3820 ± 0.6234	45.8152 ± 0.4322	47.8320 ± 0.1228
B-ESBMV (11 beams)	22.4380 ± 1.4057	13.4036 ± 0.1525	13.7640 ± 0.0764
B-ESBMV (9 beams)	18.4800 ± 0.3014	11.6174 ± 0.0246	12.3020 ± 0.0622
B-ESBMV (5 beams)	16.8160 ± 0.0789	10.5626 ± 0.0714	11.2080 ± 0.0460

DAS = delay-and-sum; MV = minimum variance; ESBMV = eigenspace-based minimum variance; B-ESBMV = beam-domain eigenspace-based minimum variance.

high as the theoretical derivation; it is a long-term topic for future research to ultimately implement the ESBMV beamformer.

VI. CONCLUSION

We have successfully applied the beam-domain ESBMV beamformer to medical ultrasound imaging to decrease the high computational loads caused by the inversion and eigen-decomposition of the covariance matrix. We demonstrate the feasibility of introducing the beamspace algorithm into the ESBMV beamformer. We form the transform matrix based on the spatial spectrum, with which the dimensions of the covariance matrix can be greatly reduced. From the imaging results of the point scatter and cyst phantom using both the simulated and experimental data, we can draw the conclusion that the proposed method could effectively decrease the computational complexity of the ESBMV beamformer, and it can provide performance comparable to the ESBMV beamformer.

REFERENCES

[1] J. Capon, "High-resolution frequency-wavenumber spectrum analysis," *Proc. IEEE*, vol. 57, no. 8, pp. 1408–1418, Aug. 1969.

[2] J. A. Mann and W. F. Walker, "A constrained adaptive beamformer for medical ultrasound: Initial results," in *Proc. IEEE Ultrasonics Symp.*, 2002, vol. 2, pp. 1807–1810.

[3] M. Sasso and C. Cohen-Bacrie, "Medical ultrasound imaging using the fully adaptive beamformer," in *Proc. IEEE Int. Conf. Acoustics, Speech, and Signal Processing*, 2005, vol. 2, pp. 489–492.

[4] J.-F. Synnevåg, A. Austeng, and S. Holm, "Adaptive beamforming applied to medical ultrasound imaging," *IEEE Trans. Ultrason. Ferroelectr. Freq. Control*, vol. 54, no. 8, pp. 1606–1613, Aug. 2007.

[5] I. K. Holfort, F. Gran, and J. A. Jensen, "Broadband minimum variance beamforming for ultrasound imaging," *IEEE Trans. Ultrason. Ferroelectr. Freq. Control*, vol. 56, no. 2, pp. 314–325, Feb. 2009.

[6] C.-I. C. Nilsen and S. Holm, "Wiener beamforming and the coherence factor in ultrasound imaging," *IEEE Trans. Ultrason. Ferroelectr. Freq. Control*, vol. 57, no. 6, pp. 1329–1346, Jun. 2010.

[7] P.-C. Li and M.-L. Li, "Adaptive imaging using the generalized coherence factor," *IEEE Trans. Ultrason. Ferroelectr. Freq. Control*, vol. 50, no. 2, pp. 128–141, Feb. 2003.

[8] B. M. Asl and A. Mahloojifar, "Eigenspace-based minimum variance beamforming applied to medical ultrasound imaging," *IEEE Trans. Ultrason. Ferroelectr. Freq. Control*, vol. 57, no. 11, pp. 2381–2390, Nov. 2010.

[9] J.-L. Yu and C.-C. Yeh, "Generalized eigenspace-based beamformers," *IEEE Trans. Signal Process.*, vol. 43, no. 11, pp. 2453–2461, Nov. 1995.

[10] S. Mehdizadeh, T. Johansen, and S. Holm, "Eigenspace based minimum variance beamforming applied to ultrasound imaging of acoustically hard tissues," *IEEE Trans. Med. Imag.*, vol. 31, no. 10, Oct. 2012.

[11] X. Zeng, C. Chen, and Y.-Y. Wang, "Eigenspace-based minimum variance beamformer combined with Wiener postfilter for medical ultrasound imaging," *Ultrasonics*, vol. 52, no. 8, pp. 996–1004, Dec. 2012.

[12] F. Vignon and M. R. Burcher, "Capon beamforming in medical ultrasound imaging with focused beams," *IEEE Trans. Ultrason. Ferroelectr. Freq. Control*, vol. 55, no. 3, pp. 619–628, Mar. 2008.

[13] J.-F. Synnevåg, S. Holm, and A. Austeng, "A low complexity data-dependent beamformer," in *Proc. IEEE Ultrasonics Symp.*, 2008, pp. 1084–1087.

[14] B. M. Asl and A. Mahloojifar, "A low-complexity adaptive beamformer for ultrasound imaging using structured covariance matrx," *IEEE Trans. Ultrason. Ferroelectr. Freq. Control*, vol. 59, no. 4, pp. 660–667, Apr. 2012.

[15] C.-I. C. Nilsen and I. Hafizovic, "Beamspace adaptive beamforming for ultrasound imaging," *IEEE Trans. Ultrason. Ferroelectr. Freq. Control*, vol. 56, no. 10, pp. 2187–2197, Oct. 2009.

[16] I. K. Holfort, F. Gran, and J. A. Jensen, "Plane wave medical ultrasound imaging using adaptive beamforming," *in Proc. 5th IEEE Sensor Array and Multichannel Signal Proc.*, 2008, pp. 288–292.

[17] J. Lu, "2D and 3D high frame rate imaging with limited diffraction beams," *IEEE Trans. Ultrason. Ferroelectr. Freq. Control*, vol. 44, no. 4, pp. 839–856, Oct. 1997.

[18] P. Kruizinga, F. Mastik, N. D. Jong, A. F. W. van der Steen, and G. V. Soest, "Plane-wave ultrasound beamforming using a nonuniform fast Fourier transform," *IEEE Trans. Ultrason. Ferroelectr. Freq. Control*, vol. 59, no. 12, pp. 2684–2691, Dec. 2012.

[19] J. Butler and R. Lowe, "Beam forming matrix simplifies the design of electronically scanned antennas," *Electron. Des.*, vol. 9, pp. 120–133, Apr. 1961.

[20] J. A. Jensen, "Field: A program for simulating ultrasound systems," *Med. Biol. Eng. Comput.*, vol. 34, suppl. 1, pt. 1, pp. 351–353, 1996.

[21] M. O'Donnell and S. W. Flax, "Phase-aberration correction using signals from point reflectors and diffuse scatterers: Measurements," *IEEE Trans. Ultrason. Ferroelectr. Freq. Control*, vol. 35, no. 6, pp. 768–774, Nov. 1988.

[22] G. H. Golub and C. F. Van-Loan, *Matrix Computations*, 3rd ed., Baltimore, MD: Johns Hopkins University Press, 1996.

[23] K.-B. Yu, "Recursive updating the eigenvalue decomposition of a covariance matrix," *IEEE Trans. Signal Process.*, vol. 39, no. 5, pp. 1136–1145, 1991.